

## Computational Predictions of 1-Octanol/Water Partition Coefficient for Imidazolium based Ionic Liquids.

Ganesh Kamath,<sup>\*a</sup> Navendu Bhatnagar<sup>b</sup>, Gary A. Baker<sup>a</sup>, Sheila N. Baker<sup>c</sup> and Jeffrey J. Potoff<sup>b</sup>

**Table 1** Comparison of the free energy of hydration, 1-octanol/water partition coefficient predicted using ABF–MD simulations at 298 K and experiment.

Ionic Liquid	$\Delta G^{HYD}$ (kcal.mol <sup>-1</sup> )	$\Delta G^{SOLV}$ dry octanol (kcal.mol <sup>-1</sup> )	$\Delta G^{SOLV}$ wet octanol (kcal.mol <sup>-1</sup> )	Log $K_{ow}$ Sim.	Log $K_{ow}$ (Wet octanol) Sim.	Log $K_{ow}$ Expt.
[BMIM] [NTf <sub>2</sub> ]	-19.96 ± 0.2 <b>(-14.5,-18.7)*<sup>1</sup></b>	-19.44 ± 0.2	-19.60 ± 0.2	-0.38 ± 0.2	-0.26 ± 0.3	-0.50, - 0.58(- 0.96 to - 0.208) <sup>2</sup>
[BMIM] [TfO]	-27.90 ± 0.3	-24.57 ± 0.3	-25.15 ± 0.3	-2.44 ± 0.3	-1.82 ± 0.3	-1.61 <sup>3</sup>
[BMIM] [PF <sub>6</sub> ]	-27.42 ± 0.3	-23.87 ± 0.2	-25.28 ± 0.3	-2.59 ± 0.3	-1.55 ± 0.3	-1.72, <sup>3</sup> -1.66, <sup>3</sup> -2.39 <sup>4</sup>
[BMIM] [BF <sub>4</sub> ]	-27.97 ± 0.3	-25.02 ± 0.2	-24.68 ± 0.3	-2.14 ± 0.3	-2.40 ± 0.3	-2.40, -2.52
[BMIM] [CH <sub>3</sub> COO]	-31.02 ± 0.3	-27.05 ± 0.2	-27.07 ± 0.2	-2.90 ± 0.6	-2.89 ± 0.6	-2.77 <sup>3</sup>
[BMIM] [dca]	-25.93 ± 0.2	-23.35 ± 0.2	-23.27 ± 0.3	-1.88 ± 0.3	-1.94 ± 0.2	-2.32 <sup>5</sup>

**\* Experimental free energy of hydration.**

### Methods

Adaptive biasing force (ABF) method is a technique developed by Darve *et al.*<sup>6-8</sup> to calculate the free energy difference of certain chemical or biological processes along generalized reaction coordinates in the system of interest. This method is a combination of probability density and constraint force methods, and is based on the thermodynamic integration of average force acting on coordinates, which is unconstrained.<sup>6</sup> As a part of ABF algorithm, an external biasing force, estimated locally from the sampled conformations of the system and updated continuously, is applied at each step to facilitate the system in overcoming significant energy barriers along the reaction coordinate. This allows the system to evolve freely without constraints, enabling the simulation to visit multiple states separated by high free energy barriers and improving sampling long the reaction coordinate. The theoretical foundation of this method is based on Equation 1, which is a modified version of the expression proposed by Darve and Pohorille<sup>6, 7</sup> for the effective force ( $F^u$ ) acting on the reaction coordinate ( $\xi$ ),

$$F_{\xi}^u = m_{\xi} \frac{d^2 \xi}{dt^2} + \frac{1}{\beta} \sum_{k=1}^{3M} \frac{1}{m_k} \frac{d\xi}{dx_k} \frac{dm_{\xi}}{dx_k} \quad (1)$$

where  $m_k$  are generalized masses associated with generalized coordinates represented by  $x_k$ .

The average of this applied force is equal and opposite to the mean force acting on  $\xi$  and cancels the free energy derivative computed for small intervals of reaction coordinate  $\xi$  so that the system can evolve and overcome free energy barriers.

$$\left\langle \frac{\partial H}{\partial \xi} \right\rangle_{\xi} = -\langle F_{\xi}^u \rangle_{\xi} \quad (2)$$

The Helmholtz free energy  $A$  at constant temperature  $T$ , constant volume  $V$  and number of particles  $N$  is given by:

$$A(N, V, T) = -k_b T \log Z(N, V, T) \quad (3)$$

where  $Z$  is the canonical partition function and  $k_b$  is the Boltzmann's constant.

The free energy as a function of the reaction coordinate can be written as:

$$A(N, V, T, \xi) = -k_b T \log \frac{\int \exp[-\beta H(x, p)] \delta(\xi(x) - \xi_o) dx dp}{\Lambda^{3M} N!} \quad (4)$$

where  $\Lambda$  is the thermal wavelength and  $p$  is the conjugate momenta of position coordinate  $x$ . It is more convenient to compute the free energy difference  $\Delta A_{a \rightarrow b}$  between state A and B for a system. The states A and B are based on the reaction coordinate which is a function of the particle position.

$$\Delta A_{a \rightarrow b} = \int_{\xi_a}^{\xi_b} \frac{dA(\xi)}{d\xi} d\xi \quad (5)$$

The first derivative of the free energy is related to the partial derivative of the Hamiltonian of the system with the reaction coordinate<sup>9</sup> and therefore based on Equation 5 can be related to the constraint force acting along the reaction coordinate

$$\Delta A_{a \rightarrow b} = \int_{\xi_a}^{\xi_b} \frac{dA(\xi)}{d\xi} d\xi = \int_{\xi_a}^{\xi_b} \left\langle \frac{dH(\xi)}{d\xi} \right\rangle_{\xi} d\xi = \int_{\xi_a}^{\xi_b} -\langle F_{\xi}^u \rangle_{\xi} d\xi \quad (6)$$

Further details of the ABF method and formulation including the implementation in NAMD<sup>10</sup> molecular dynamics package can be found in these publications<sup>6-9, 11-14</sup>. The Helmholtz free energy  $A$  obtained from NVT ensemble simulations is in close approximation to the Gibbs free energy  $G$  in condensed phase.<sup>15</sup> The Gibbs free energy difference is used to compute the free energy of hydration and partition function.

### **Intermolecular Potential**

The force field developed by Lopes and co-workers based on the OPLS/AMBER framework was used to model the dialkylimidazolium cation<sup>16, 17</sup> and anions ([NTf<sub>2</sub>]<sup>18, 19</sup>, [TfO]<sup>18</sup>, [PF<sub>6</sub>]<sup>16, 18</sup>, [BF<sub>4</sub>]<sup>20</sup>, [CH<sub>3</sub>COO]<sup>21</sup> and [dca]<sup>22</sup>). This is a very widely used force field for ionic liquids based on the 12-6 Lennard Jones model and point charges and predicts the thermodynamic properties with excellent agreement with experiment.

### **Simulation Details**

Three different configurations were generated for the required calculations; water|vacuum (S1) and 1-octanol|vacuum (S2) systems for the indirect transfer (IT) approach. For systems S1 and S2, a rectangular simulation cell was used, with dimensions 30 × 30 × 60 Å, with the condensed phase occupying a region approximately 30 × 30 × 30 Å. This cell was extended to 150 Å in the z-direction with a 90 Å vacuum region. The vacuum region is necessary to prevent interactions of the solute with the condensed phases through periodic boundary conditions. The number of molecules in each box was selected to reproduce the density of water or 1-octanol predicted by *NPT* simulations at 1 atm and 298 K for a specific potential truncation (14 Å). For systems utilizing a 14 Å cut-off, 102 and 896 1-octanol and water molecules were used, respectively. It should be noted that the TraPPE force field was developed using an analytical tail correction for Lennard-Jones interactions, and therefore it is expected that the predictions of simulations using a truncated potential will differ slightly from the original parameterization. In this case, the predicted densities for 1-octanol at 298 K and 1 atm was 0.814 (r<sub>cut</sub> = 14 Å), which are in reasonable agreement with the experimental value of 0.826, but slightly less than predicted by the TraPPE force field when used with analytical tail corrections for the Lennard-Jones interactions.

The reaction coordinate for the determination of free energy changes was defined as the distance between the center of mass of the solute (COMS) under study and center of mass of the condensed phase (COMCP). In the initial system setup, the COMS was placed at approximately the COMCP. Over the course of simulation, the reaction coordinate spanned a distance of 30.0 Å from the center of mass of the condensed phase to the center of the vacuum region, or center of mass of the 1-octanol phase. To reduce the statistical error of the calculations, the reaction pathway was divided into five equally sized non-overlapping windows of 5.0 Å. To generate the

initial configurations for each window, a single 5 ns ABF run was performed spanning the complete reaction pathway from 0.0 Å to 30.0 Å after heating and equilibration of the system. Coordinates from the trajectory of this simulation were saved periodically to generate five initial coordinate files for the five windows. Force statistics were stored in bins of width 0.05 Å. The biasing force was applied after 500 samples were collected in each bin. To keep the solute within the specified window, a harmonic force with a magnitude of 10.0 kcal/mol/Å was applied on the upper and lower boundary of the window along the z-axis of the simulation cell. A final production run of 10 ns for each window was performed.

Molecular dynamics simulations were performed with NAMD version 2.7b3<sup>10</sup>. Initial configurations for each system were generated with Packmol<sup>23</sup>. Energy minimization was performed on all systems for 500 steps using the steepest decent technique. Systems were equilibrated over a time period of 2.0 ns in isobaric–isothermal ensemble at 1.0 atm and 298 K, followed by the ABF-MD calculation in *NVT* ensemble. For all calculations, the temperature was maintained at 298.0 K using Langevin dynamics. For initial *NPT* simulations, used to determine the density of each system, constant pressure was maintained at 1.0 atm using the Nose–hoover algorithm<sup>24,25</sup>. A timestep of 2.0 fs was used for the integration of Newton's equation of motion. Periodic boundary conditions were used in all the three spatial coordinates. Long range electrostatic interactions were calculated with particle–mesh Ewald algorithm<sup>26, 27</sup>. A switching function was applied for all Lennard–Jones interactions at 12.5 Å for 14.0 Å cut-off. Data were analyzed using VMD<sup>28</sup>. Statistical errors were estimated from the standard deviation of the predicted free energies generated from three to five unique simulations.

**Figure S1** Free energy of hydration and solvation of the six imidazolium based ILs predicted using ABF–MD simulations at 298 K.

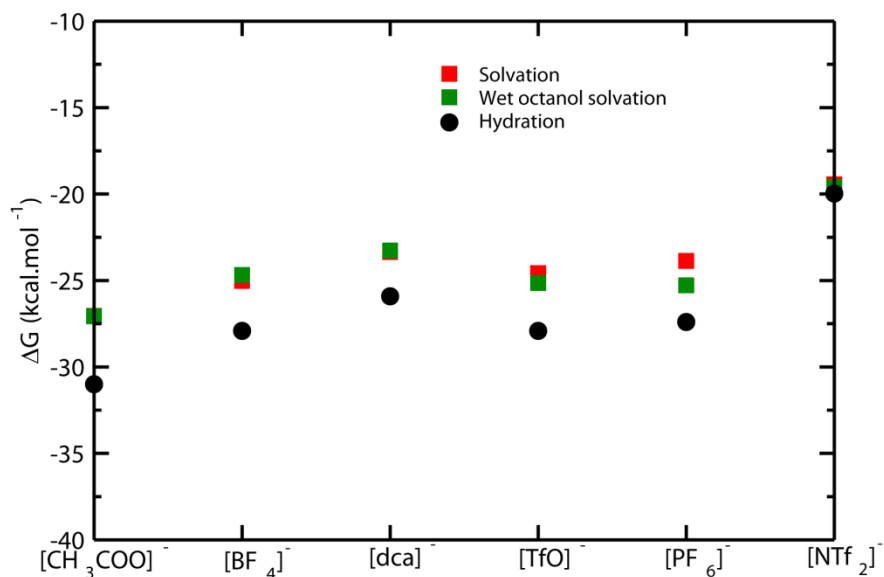
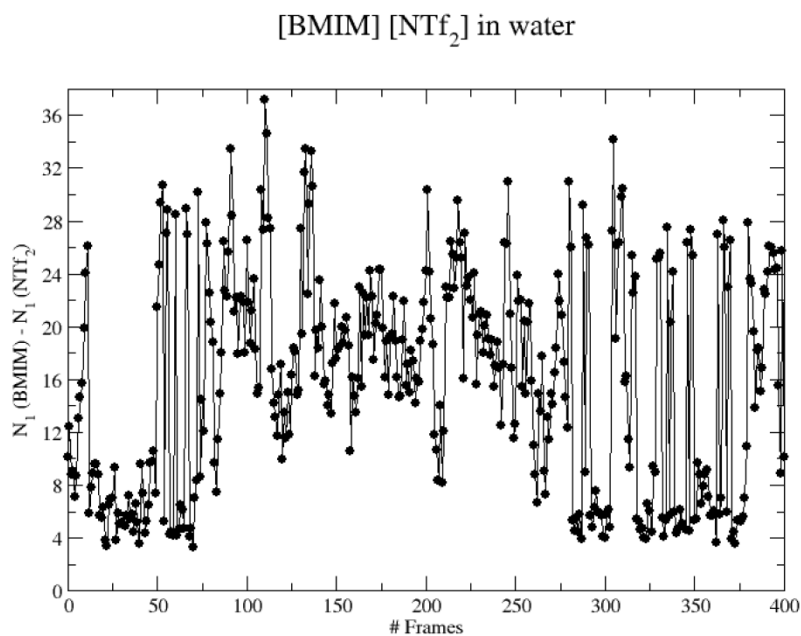


**Figure S2** Distance between cation ([bmim]) and anion ([NTf<sub>2</sub>]) in water during ABF simulation as a function of time step.



1. M. G. Freire, P. J. Carvalho, R. L. Gardas, I. M. Marrucho, L. M. N. B. F. Santos and J. A. P. Coutinho, *J.Phys.Chem. B*, 2008, **112**, 1604-1610.

2. L. Ropel, L. S. Belvèze, S. N. V. K. Aki, M. A. Stadtherr and J. F. Brennecke, *Green Chem.*, 2005, **7**, 83-90.
3. C.-W. Cho, U. Preiss, C. Jungnickel, S. Stolte, J. Arning, Ranke, A. J. Klamt, I. Krossing and J. Thoming, *J. Phys. Chem. B*, 2011, **115**, 6040-6050.
4. J. L. Kaar, A. M. Jesionowski, J. A. Berberich, R. Moulton and A. J. Russell, *J. Am. Chem. Soc.*, 2003, **125**, 4125-4131.
5. H. Zhao, G. A. Baker, Z. Songa, O. Olubajo, L. Zandersa and S. M. Campbell, *J. Mol. Catal.*, 2009, **57**, 149-157.
6. E. Darve and A. Pohorille, *J. Chem. Phys.*, 2001, **115**, 9169-9183.
7. E. Darve, M. A. Wilson and A. Pohorille, *Mol. Sim.*, 2002, **28**, 113-144.
8. D. Rodriguez-Gomez, E. Darve and A. Pohorille, *J Chem Phys*, 2004, **120**, 3563.
9. E. Darve, David Rodríguez-Gómez and A. Pohorille, *J Chem Phys*, 2008, **128**, 144120.
10. J. C. Phillips, R. Braun, W. Wang, J. Gumbart, E. Tajkhorshid, E. Villa, C. Chipot, R. D. Skeel, L. Kale and K. Schulten, *J. Comp. Chem.*, 2005, **26**, 1781-1802.
11. C. Chipot and J. Henin, *J Chem Phys*, 2005, **123**.
12. J. Henin and C. Chipot, *J. Chem. Phys.*, 2004, **121**, 2904-2914.
13. J. Henin, G. Fiorin, C. Chipot and M. L. Klein, *J. Chem. Theo. Comput.*, 2010, **6**, 35-47.
14. C. Chipot and A. Pohorille, *Free Energy Calculations*, Springer, 2007.
15. M. Buhl and G. Wipff, *Chemphyschem*, 2011, **12**, 3095-3105.
16. J. Lopes, J. Deschamps and A. Padua, *J. Phys. Chem. B*, 2004, **108**, 2038-2047.
17. J. N. C. Lopes, J. Deschamps and A. A. H. Padua, *J. Phys. Chem. B*, 2004, **108**, 11250.
18. J. N. C. Lopes and A. I. A. H. Pa'dua, *J. Phys. Chem. B*, 2004, **108**, 16893-16898.
19. K. Shimizu, D. Almantariotis, Margarida F. Costa Gomes and A. I. A. H. P. d. J. N. C. Lopes, *J. Phys. Chem. B*, 2010, **114**, 3592-3600.
20. Z. Liu, S. Huang and W. Wang, *J. Phys. Chem. B*, 2004, **108**, 12978-12989.
21. Hanbin Liu, Kenneth L. Sale, B. A. Simmons and S. Singh, *J. Phys. Chem. B*, 2011, **115**, 10251-10258.
22. J. N. C. Lopes and A. I. A. H. Pa'dua, *J. Phys. Chem. B*, 2006, **110**, 19586-19592.
23. L. Martinez, R. Andrade, E. G. Birgin and J. M. Martinez, *J Comput Chem*, 2009, **30**, 2157-2164.
24. S. E. Feller, Y. H. Zhang, R. W. Pastor and B. R. Brooks, *J Chem Phys*, 1995, **103**, 4613-4621.
25. G. J. Martyna, D. J. Tobias and M. L. Klein, *J. Chem. Phys.*, 1994, **101**, 4177.
26. T. Darden, D. York and L. Pedersen, *J Chem Phys*, 1993, **98**, 10089-10092.
27. U. Essmann, L. Perera, M. L. Berkowitz, T. Darden, H. Lee and L. G. Pedersen, *J Chem Phys*, 1995, **103**, 8577-8593.
28. W. Humphrey, A. Dalke and K. Schulten, *J Mol Graphics*, 1996, **14**, 33-&.